

INTERLAMINAR FRACTURE AND IMPACT DAMAGE ASSESSMENT BY ELECTRICAL RESISTIVITY TOMOGRAPHY IN GFRP LAMINATES WITH CONDUCTIVE NANOPARTICLES

L. Ye^{1,*}, D. Zhang^{1,2}, D. Wang^{1,3}

¹Centre for Advanced Materials Technology, School of Aerospace, Mechanical and Mechatronic Engineering, The University of Sydney, NSW 2006, Australia

²State Key Laboratory of Multi-phase Complex Systems, Institute of Process Engineering, Chinese Academy of Sciences, Beijing 100190, China

³Beijing Aeronautical Science & Technology Research Institute, Beijing 100083, China
lin.ye@sydney.edu.au

Keywords: Interlaminar fracture, impact damage assessment, GFRP, conductive nanoparticles.

Abstract

In this study, GF/EP composite laminates with an epoxy matrix modified by carbon black (CB) nanoparticles of 2.0 wt% and copper chloride (CC) were manufactured using the vacuum assisted resin infusion (VARI) method. The addition of CB nanoparticles and CC substantially improves electrical conductivity of GF/EP composites in all three principal directions with percolation network of CB nanoparticles. The addition of CB nanoparticles increases both initiation and propagation values of modes I and II interlaminar fracture toughness of GF/EP composite laminates. The change in electrical resistance was used as a damage index to monitor delamination growth. With the damage index for individual pathways of a network in GF/EP quasi-isotropic laminates with CB and CC. An electrical resistivity tomography method was successfully developed to locate and quantitatively assess growth of transverse impact damage in the GF/EP composite laminates.

1 Introduction

With several decades of development, glass fibre reinforced polymer (GFRP) composites have succeeded as structural materials in various applications. However, due to the brittle nature of the thermosetting matrix and reinforcing fibres, damage in these composites, in particular delamination or matrix cracking, is of major practical concern. Generally, the extent of damage in composite materials can be assessed using non-destructive inspection (NDI) procedures, including ultrasonic C-scan, enhanced radiography, thermography, acoustic emission. Many new NDI methods are being employed, enabling potential *in-situ* or real time damage assessment, such as using distributed piezoelectric or FBG transducers with guided ultrasonic wave signals. Damage detection based on electrical impedance has some interesting features, and it relies on changes in conductivity, which are related to location and severity of damage. For this method to be applicable for GFRP composites, the first challenge is to induce good electrical conductivity in GFPRs made of dielectric fibres and matrix. The most commonly used method is to modify the polymer matrix using conductive nanoparticles. Thostenson and Chou reported an approach using carbon nanotubes *in-situ* sensing to detect

localized damage in a glass fibre composite of mechanically fastened joints [1]. Böger et al. demonstrated the good potential of electrical conductivity methods for sensing stress/strain and damage in FRPs with carbon nanoparticle-modified matrices [2]. Further studies of sensing impact damage of carbon fibre-epoxy laminates in real-time have been conducted by measuring the electrical resistance of the upper surface (the surface receiving the impact), or of the through-thickness away from the impact region, using distributed through-width electrodes [3-5]. Dielectric electrical resistance measurement has also been utilised in GF/EP laminate composite for load or strain monitoring to evaluate the evolution of damage, modifying the matrices with carbon nanotubes to form conductive networks [2, 6].

In this study, GF/EP composite laminates with an epoxy matrix modified by carbon black (CB) nanoparticles and copper chloride (CC) were manufactured by the vacuum assisted resin infusion (VARI) technique. A new method of electrical resistivity tomography was developed to assess low-velocity transverse impact damage in GF/EP composite laminates.

Experimental

2.1 Materials

Super conductive carbon black (Printex[®] XE2) was obtained from Degussa Australia Pty Ltd, with a nominal particle size of 35nm and a BET surface area of 950m²/g. A diglycidyl ether of bisphenol A (DGEBA) based epoxy resin (Huntsman Advanced Materials Ltd) was used as the matrix for the composites. Piperidine hardener and copper chloride (CuCl₂, anhydrous), each with a purity of >97%, were obtained from Sigma-Aldrich Australia. Unidirectional glass stitched fabrics (F02190) with a unit weight of 907g/m² per layer were purchased from FGI (Fiberglass International Australia).

2.2 Modified epoxies and GF/EP laminates

The GF/EP laminates were prepared using a VARI technique in combination with hot pressing. A stack of [0]₁₀ of unidirectional GF fabrics was laid up with a polyimide film of 50 µm in thickness at one end, which was coated with a release agent and embedded in the centre plane as a starter crack for Modes I and II interlaminar fracture toughness tests. For a drop-weight impact event, a balanced, symmetric stack of GF fabrics was laid up with a stacking sequence of [45/0/-45/90]_s.

A master batch epoxy resin, containing 10.0 wt% CB, was prepared through a planetary ball mill, Pulverisette 5 (Fritsch, Germany), and diluted into the epoxy resin with 2.0 wt% CB. A solution of piperidine and CC was added at 100 °C and stirred with mechanical stirrer for 1 minute. The ratio of epoxy resin to hardener was 20:1 and the concentration of CC in the resin was adjusted to 3×10⁻⁶ mol/g. Finally, the laminate was fabricated through VARI with a vacuum of 0.1 MPa in the sealed vacuum bag, followed by hot pressing at a pressure of 0.4 MPa and at 120 °C for 16 hrs. This process resulted in a GF/EP laminate with a high fibre volume fraction of 61%.

2.3 Delamination characterisation

G_{IC} was measured using the double cantilever beam (DCB) test on the basis of ASTM D 5528, calculated according to the modified beam theory (MBT) method. G_{IIC} was measured

using the end notched flexure (ENF) test according to an ESIS protocol [7] in a three point bending configuration, determined according to the corrected beam theory.

Measurements of volume resistance (R) were conducted using a direct-reading instrument, a digital multimeter (Agilent 34401A 6 1/2 Digital Multimeter), at ambient temperature. Resistivity (ρ) was calculated according to

$$\rho = \frac{RA}{L} \tag{1}$$

where A is the cross-sectional area and L is the length of the specimen.

The resistance changes of GF/EP laminates during Modes I and II interlaminar fracture testing were monitored at a sampling rate of 5 Hz. The upper and lower surfaces were painted as electrodes using silver conductive paint of 5 mm in width, from the tip of the precrack. The resistance change (δ) was calculated by $\delta = (R - R_0)/R_0$, where R_0 is the benchmark resistance before damage occurs.

2.4 Damage Assessment

The drop-weight impact test was performed using an impact device according to ASTM D 7136/D 7136 M-05. The total mass of the impactor was 5.5 kg, and it had a smooth hemispherical strip tip with a diameter of 15.9 mm. The ratio of impact energy to specimen thickness was specified as 6.7 J/mm. GF/EP laminate samples were impacted by 50%, 100%, 150% of standard energy, respectively.

Measurements of the electrical resistance (R) were conducted before and after each impact event, based on in-plane measurements with a 9x9 matrix of contact points along the edges of the GF/EP laminates, with intervals of 10 mm, forming multiple in-plane conductive pathways, shown in Fig. 1.

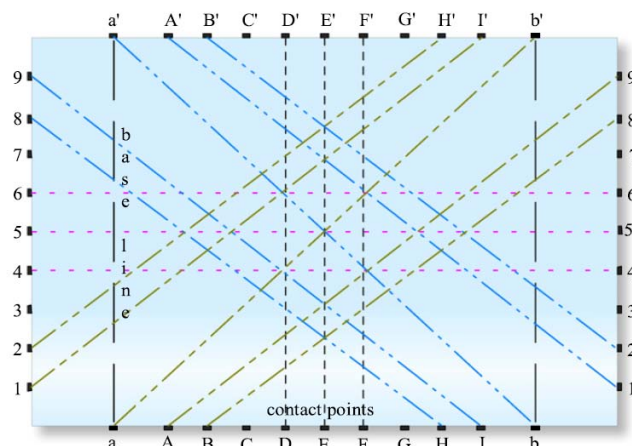


Fig.1 Schematics of conductive in-plane pathways for damage detection in GF/EP laminates

The damage can be evaluated using a tomography approach. It is based on the following assumptions: (1) damage (e.g. matrix cracks and delamination) breaks down electrical conductive pathways; (2) the growth of damage increases electrical resistance; and (3) for a particular conductive pathway, the greater the change in electrical resistance, the closer the pathway is to the damage. In this way, a network of pathways can construct an in-plane image

of damage using a tomography approach, using an analogy to the approaches adopted in constructing an image of damage using a damage index defined from ultrasonic wave signals captured from an actuator-sensor network [8].

Assuming that there are N conductive pathways in total involved for constructing the in-plane image of damage, the accumulated and weighted change in electrical resistance at position (x,y) in the monitoring area can be written as:

$$P(x,y) = \sum_{k=1}^N p_k(x,y) = \sum_{k=1}^N \delta_k \cdot W_k[R_k(x,y)] \quad (2)$$

where δ_k is the damage index for the *k*-th conductive pathway, defined by Equations (2). $W_k[R_k(x,y)]$ is the weight given to the damage signature for the *k*-th conductive pathway at (x,y). It is dependent on parameter, $R_k(x,y)$, which is defined as the relative distance from (x,y) to the *k*-th sensing path:

$$R_k(x,y) = \frac{D_{a,k}(x,y) + D_{s,k}(x,y)}{D_k} - 1 \quad (3)$$

where D_k is the distance between the beginning and end for the *k*-th conductive pathway, while $D_{a,k}(x,y)$ and $D_{s,k}(x,y)$ are the distances between (x,y) and the beginning and end, respectively. The weight is expected to increase with a decrease in the relative distance, indicating that a grid closer to the conductive pathway is more relevant to perception of the damage. In particular, the weight peaks at 1.0 when a grid falls on the conductive pathway. It is assumed that $W_k[R_k(x,y)]$ follows a simple linear distribution function when (x,y) is located inside the affected zone of the *k*-th conductive pathway (specified by a scaling parameter, β was set as 0.05 in this study); otherwise, $W_k[R_k(x,y)]$ equals to zero. The weight function can be thus detailed as [8]:

$$W_k[R_k(x,y)] = \begin{cases} 1 - R_k(x,y)/\beta, & R_k(x,y) < \beta \\ 0, & R_k(x,y) \geq \beta \end{cases} \quad (4)$$

In this way, the location with intensity values for the presence of damage above a specified threshold can be defined as the damage area. In particular, the grid with the highest intensity value indicates the centre of the identified damage.

For comparison, damage in the GF/EP laminates after impact with 100% and 150% standard energy was screened using C-Scan with a frequency of 5 MHz and a pitch of 1 mm for comparison

3. Results and Discussion

3.1 Electrical resistivity

The electrical resistivity of the GF/EP composites in the fibre, transverse and through-thickness directions surpassed the percolation threshold when the epoxy matrix was modified by 2.0 wt% CB, and the electrical resistivity was further decreased by nearly an order of magnitude with the use of 2.0 wt% CB in combination with CC, shown in Table 1. The function of CC in improving the conductivity of the epoxy matrix can be explained using the theory of colloidal dispersion – an increase in the ionic concentration helps achieve permanent stable particle contacts and induces a conductive cluster network [9].

3.2 Interlaminar fracture toughness

Table 2 summarises the interlaminar fracture toughness of the GF/EP laminates. $G_{IC, ini}$ and $G_{IC, prop}$ were increased by 13.3% and 8.6% respectively when the GF/EP laminate was modified using 2.0 wt% CB, and these properties did not change greatly when CC was also added. For Mode II interlaminar fracture, $G_{IIC, ini}$ was increased by 22.4% and $G_{IIC, prop}$ by 18.7% for the GF/EP laminates with 2.0 wt% CB particles. However, these properties were increased by 32.6% and 31.8% respectively for the laminates with 2.0 wt% CB and CC.

Table 1 Electrical Resistivity of GF/EP composite laminates with conductive nanoparticles

GF/EP composite materials	Type	Manufacturing method	Fibre volume fraction V_f [%]	Resistivity [ohm.cm]		
				ρ_L	ρ_{Tran}	ρ_r
2.0 wt% CB	UD	VARI	61.8	1.3×10^5	5.97×10^5	1.27×10^7
2.0 wt% CB&CC	UD	VARI	60.2	2.57×10^4	8.36×10^4	3.33×10^6

Table 2 Interlaminar fracture toughness of GF/EP composites with CB nanoparticles

GF/EP laminates	Interlaminar fracture toughness			
	G_{IC} [J/m ²]		G_{IIC} [J/m ²]	
	Initiation	Propagation	Initiation	Propagation
Unidirection, Neat, $V_f = 61.9\%$	384±41	1088±106	1715±110	1845±118
2.0 wt% CB, $V_f = 61.8\%$	425±99	1181±56	2099±154	2190±144
2.0 wt% CB&CC, $V_f = 60.2\%$	436±66	1238±111	2274±305	2432±271

3.3 In-situ monitoring of delamination growth

Fig. 2 shows the change in electrical resistance during a Mode-I DCB delamination test, together with the load-displacement curve. The positions of deviation from linearity of the load-displacement curve and a clear increase in electrical resistance are marked with dashed lines. The resistance change clearly indicates the initiation and growth of delamination. In Fig.3, rapid increases are also observed in the electrical resistance change-displacement curve corresponding to the start of nonlinearity and the maximum load in the load-displacement curve for delamination onset and unstable growth. The monitoring of delamination growth is very sensitive in this case, because the electrical conductivity of GF/EP composites is not influenced by interlaminar fibre bridging.

3.4 Damage assessment using electrical resistivity tomography

Fig. 4 shows damage images constructed using in-plane electrical resistivity tomography for the GF/EP laminate with modified epoxy resins, impacted by 50%, 100% and 150% standard energy, respectively, where the intensity of the presence of damage at a location is directly related to the accumulated change of electrical resistance of individual pathways. The threshold in the change in electrical resistance was set to be 6%, which was based on the value of the change in electrical resistance for mode II delamination growth, Fig. 3. In this way, the damage area is displayed as the dark region in the images. Compared to the C-scan images of the GF/EP laminates modified using 2.0 wt% CB and CC shown in Fig. 5, the damage image from the in-plane electrical resistivity tomography seems larger. This is

because the value of intensity at individual grids was accumulated from the electrical resistance changes of individual conductive pathways.

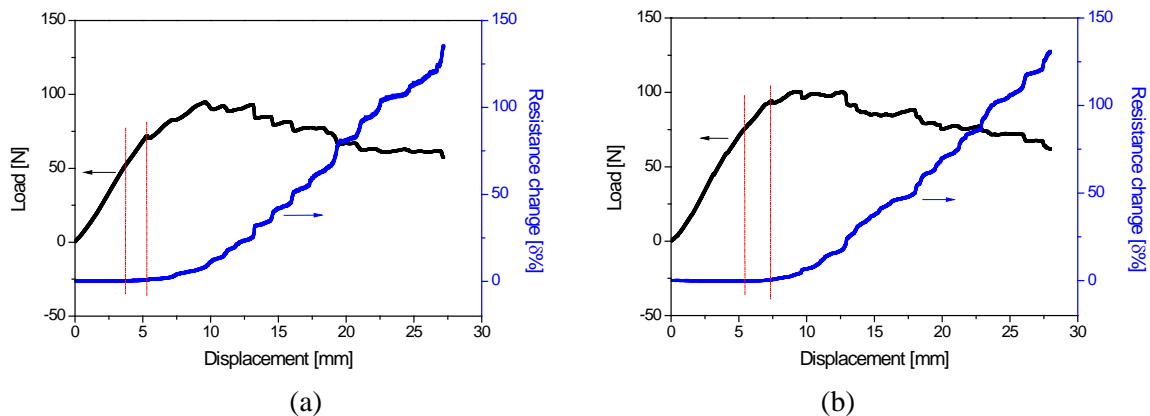


Fig.2. Load-displacement curve and change in electrical resistance with crack opening displacement for Mode I interlaminar fracture test, (a) 2.0 wt% CB, and (b) 2.0 wt% CB&CC

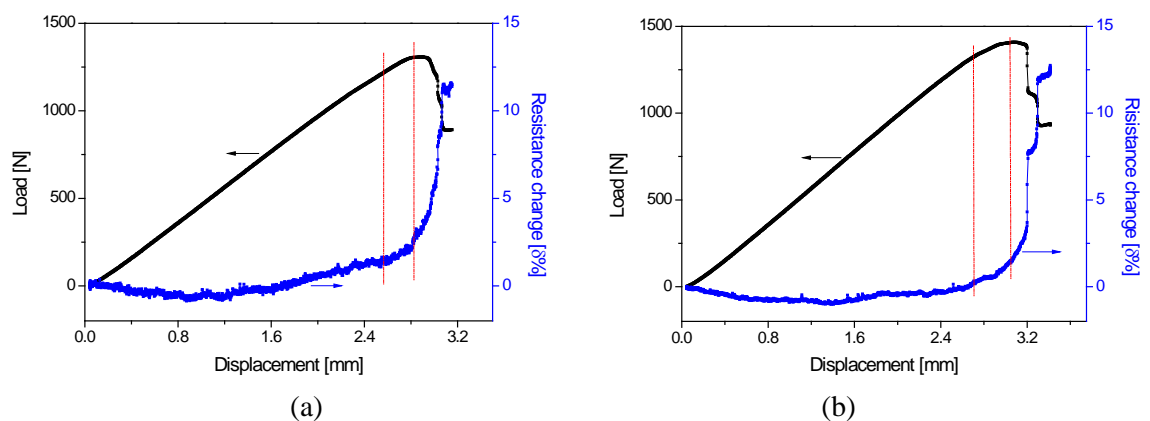


Fig.3 Load-displacement curve and change in electrical resistance with crack opening displacement for Mode II interlaminar fracture test, (a) 2.0 wt% CB, and (b) 2.0 wt% CB&CC

4. Conclusions

Unidirectional GF/EP laminate composites were manufactured using the VARI method with the epoxy matrix modified by 2.0 wt% CB particles and a small amount of CC. The CC promoted the formation of conductive networks with CB particles. The addition of CB and CC enhanced the interlaminar fracture toughness and impact damage resistance of GF/EP laminate composites.

The electrical resistivity of the GF/EP laminate composites in the fibre, transverse and through-thickness directions surpassed the percolation threshold when it was modified by 2.0 wt% CB, and the electrical resistivity further decreased by nearly an order of magnitude when using 2.0 wt% CB was used in combination with CC. The experimental results showed that the change in electrical resistance can be used to monitor the onset and growth of Modes I and II delamination.

A new method of electrical resistivity tomography was developed to access transverse impact damage in GF/EP laminates based on the changes in electrical resistance measured on a group of conductive pathways. The damage image from the in-plane electrical resistivity tomography exhibited reasonably good agreement with that in the corresponding C-scan.

Acknowledgements

Lin Ye is grateful for the research support of the Australian Research Council (ARC). The authors also acknowledge the facilities as well as scientific and technical assistance from staff at the Boeing Aerostructures Australia NDT Department.

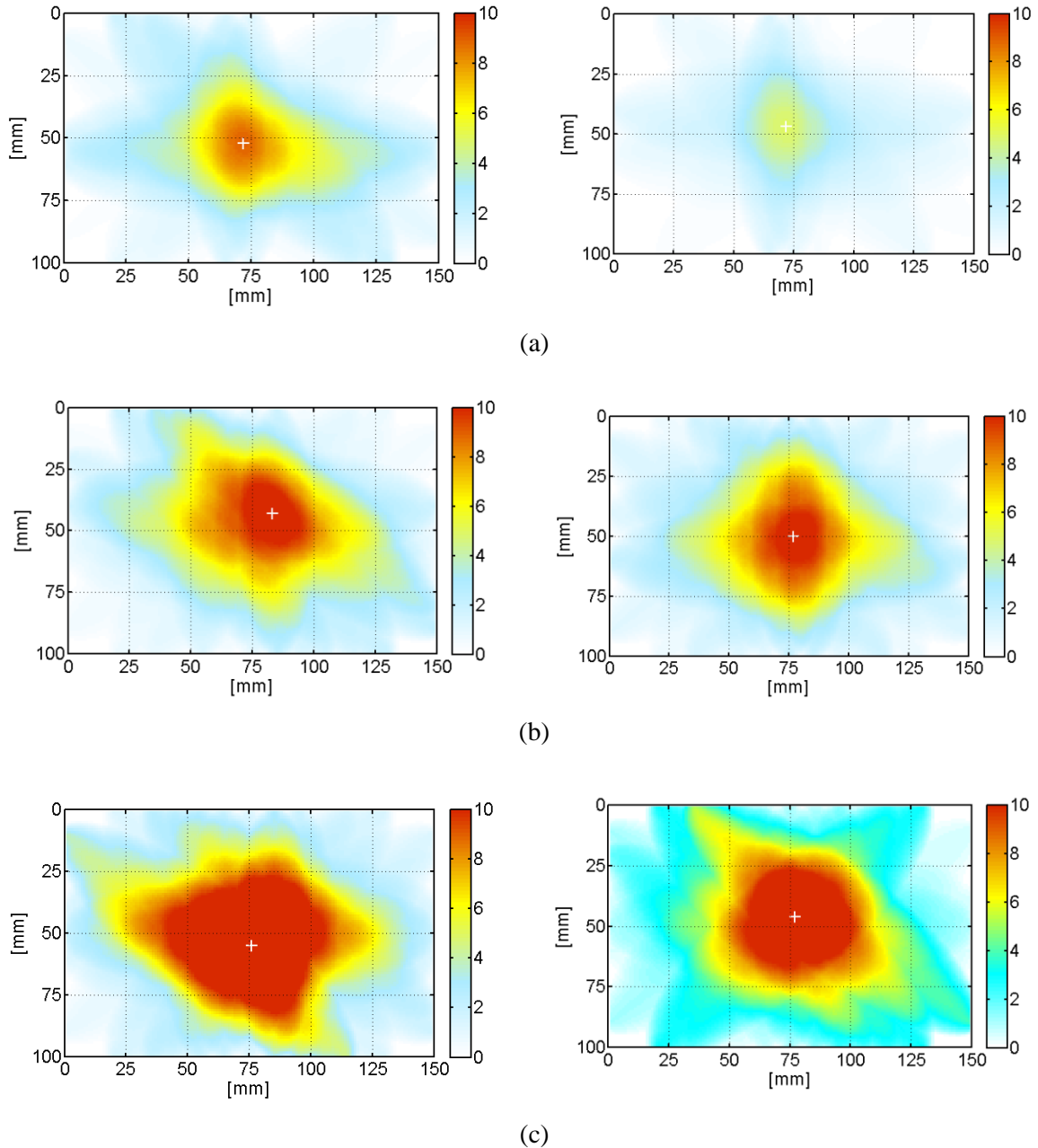


Fig.4 Impact damage assessment of GF/EP laminates (left: 2.0 wt% CB, right: 2.0 wt% CB and CC) with in-plane electrical resistivity tomography, (a) 50% standard energy, (b) 100% standard energy, and (c) 150% standard energy

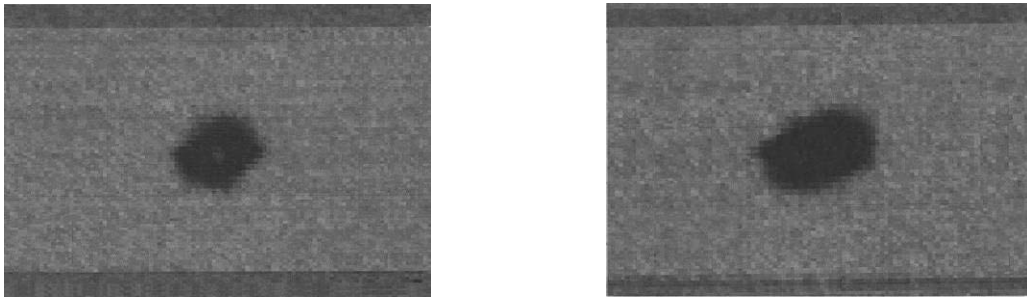


Fig.5. C-scan images of damage areas in GF/EP laminates with modified epoxy resin with 2.0 wt% CB and CC (left: 100% standard energy, and right: 150% standard energy)

References

- [1]. Thostenson ET, Chou TW. Carbon nanotube-based health monitoring of mechanically fastened composite joints. *Compos Sci Technol* 2008; 68(12):2557-61
- [2]. Böger L, Wichmann MHG, Meyer LO, Schulte K. Load and health monitoring in glass fibre reinforced composites with an electrically conductive nanocomposite epoxy matrix. *Compos Sci Technol* 2008; 68(7-8):1886-94
- [3]. Todoroki A, Tanaka M, Shimamura Y. Measurement of orthotropic electric conductance of CFRP laminates and analysis of the effect on delamination monitoring with an electric resistance change method. *Compos Sci Technol* 2002; 62(5):619-28
- [4]. Wang S, Wang D, Chung DDL. Method of sensing impact damage in carbon fiber polymer-matrix composite by electrical resistance measurement. *J Mater Sci* 2006; 41(8):2281-9
- [5]. Wang S, Chung DDL, Chung JH. Impact damage of carbon fiber polymer-matrix composites, studied by electrical resistance measurement. *Compos Part A* 2005; 36(12):1707-15
- [6]. Thostenson ET, Chou TW. Carbon nanotube networks: sensing of distributed strain and damage for life prediction and self healing. *Adv Mater* 2006; 18(21):2837-41
- [7]. ESIS-TC4, polymer and composites: protocols for interlaminar fracture testing of composites. 1992
- [8]. Wang D, Ye L, Lu Y. A probabilistic diagnostic algorithm for identification of multiple notches using digital damage fingerprints (DDFs). *Journal of intelligent Material Systems and Structures* 2009; 20(12):1439-50
- [9]. Schueler R, Petermann J, Schulte K, W Hans-Peter. Agglomeration and electrical percolation behavior of carbon black dispersed in epoxy resin. *J Appl Polym Sci* 1997; 63(13):1741-6